Title

Prader—Willi locus Snord116 RNA processing requires an active endogenous allele and neuron-specific splicing by Rbfox3/NeuN

Journal

Human Molecular Genetics, 27(23)

ISSN

0964-6906

Authors

Coulson, Rochelle L

Powell, Weston T

Yasui, Dag H

et al.

Publication Date

2018-12-01

DOI

10.1093/hmg/ddy296

Peer reviewed

Human Molecular Genetics, 2018, Vol. 27, No. 23 4051–4060

doi: 10.1093/hmg/ddy296
Advance Access Publication Date: 14 August 2018
General Article

GENERAL ARTICLE

Prader–Willi locus *Snord116* RNA processing requires an active endogenous allele and neuron-specific splicing by *Rbfox3*/NeuN

Rochelle L. Coulson[1], Weston T. Powell[1], Dag H. Yasui[1], Gayathri Dileep[1], James Resnick[2] and Janine M. LaSalle[1,*]

[1]Microbiology and Immunology, Genome Center, and MIND Institute, UC Davis School of Medicine, Davis, CA 95616, USA and [2]Molecular Genetics and Microbiology, University of Florida College of Medicine, Gainesville, FL 32601, USA

*To whom correspondence should be addressed at: Medical Microbiology and Immunology, One Shields Avenue Davis, CA 95616, USA. Tel: (530) 754-7598; Fax: (530) 752-8692; Email: jmlasalle@ucdavis.edu

Abstract

Prader–Willi syndrome (PWS), an imprinted neurodevelopmental disorder characterized by metabolic, sleep and neuropsychiatric features, is caused by the loss of paternal *SNORD116*, containing only non-coding RNAs (ncRNAs). The primary *SNORD116* transcript is processed into small nucleolar RNAs (snoRNAs), which localize to nucleoli, and their spliced host gene *116HG*, which is retained at its site of transcription. While functional complementation of the *SNORD116* ncRNAs is a desirable goal for treating PWS, the mechanistic requirements of *SNORD116* RNA processing are poorly understood. Here we developed and tested a novel transgenic mouse which ubiquitously expresses *Snord116* on both a wild-type and a *Snord116* paternal deletion (*Snord116*$^{+/-}$) background. Interestingly, while the *Snord116* transgene was ubiquitously expressed in multiple tissues, splicing of the transgene and production of snoRNAs was limited to brain tissues. Knockdown of *Rbfox3*, encoding neuron-specific splicing factor neuronal nuclei (NeuN) in *Snord116*$^{+/-}$-derived neurons, reduced splicing of the transgene in neurons. RNA fluorescence *in situ* hybridization for *116HG* revealed a single significantly larger signal in transgenic mice, demonstrating colocalization of transgenic and endogenous *116HG* RNAs. Similarly, significantly increased snoRNA levels were detected in transgenic neuronal nucleoli, indicating that transgenic *Snord116* snoRNAs were effectively processed and localized. In contrast, neither transgenic *116HG* nor snoRNAs were detectable in either non-neuronal tissues or *Snord116*$^{+/-}$ neurons. Together, these results demonstrate that exogenous expression and neuron-specific splicing of the *Snord116* locus are insufficient to rescue the genetic deficiency of *Snord116* paternal deletion. Elucidating the mechanisms regulating *Snord116* processing and localization is essential to develop effective gene replacement therapies for PWS.

Introduction

Prader–Willi syndrome (PWS) is a neurodevelopmental disorder characterized by a broad range of symptoms including hypotonia and failure to thrive in infancy followed by the onset of hyperphagia, intellectual impairment, obsessive-compulsive tendencies and sleep abnormalities including shorter sleep duration and daytime sleepiness (1). PWS is caused by paternal deficiency of the maternally imprinted 15q11-q13 locus, which encodes a long neuron-specific transcript (Fig. 1). Expression of this locus

Received: April 23, 2018. **Revised:** June 10, 2018. **Accepted:** July 3, 2018

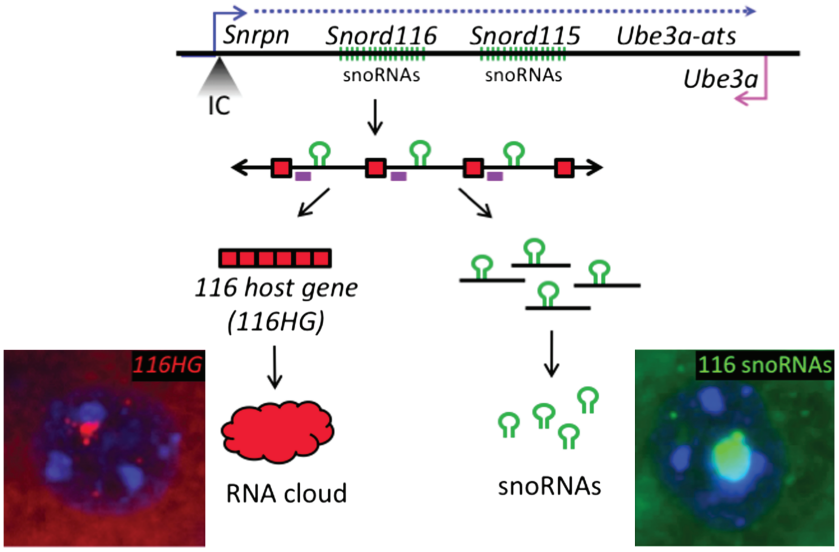

Figure 1. The PWS locus encodes a long ~1 Mb transcript containing the *Snord116* and *Snord115* snoRNA clusters. The imprinting control (IC) region is located at the 5′ end of *Snrpn*, with paternal expression of this locus extending through the *Snord116* and *Snord115* snoRNA clusters and the antisense to the maternally expressed *Ube3a* in neurons. The long paternally expressed transcript is shown in blue and maternally expressed *Ube3a* is shown in pink. The primary *Snord116* transcript is comprised of a repeating array of exons (red) flanking intron-embedded snoRNAs (green). Processing of this primary transcript produces snoRNAs from the introns of *Snord116* and the *116HG* from the spliced exons of *Snord116*. Localization of the *116HG* (red) and *Snord116* snoRNAs (green) are shown by RNA FISH (blue = DAPI). Location of *Rbfox3* binding motifs indicated on primary transcript as purple boxes.

originates at the PWS imprinting control region (IC) at the 5′ end of *SNRPN*, extends through small nucleolar RNA (snoRNA) clusters *SNORD116* (27 copies in human, >40 copies in mouse) and *SNORD115* (47 copies in human, 37 copies in mouse) and terminates antisense to the maternally expressed *UBE3A (UBE3A-ATS)* (2–5). PWS is considered a contiguous gene disorder, as most patients carry large paternal deletions of this locus; however, analyses of PWS patients have revealed that small deletions of the *SNORD116* cluster of snoRNAs are also sufficient to cause PWS (6–9). *Snord116* is processed to form two non-coding RNAs (ncRNAs): *Snord116* snoRNAs and the *Snord116* host gene *(116HG)*. *Snord116* snoRNAs are intronically embedded within the non-coding *Snord116* primary transcript, and although they currently have no known target sequence, they localize to the nucleolus in mature neurons (10–12), detectable by RNA fluorescence *in situ* hybridization (FISH) (Fig. 1). It has also been proposed that these orphan snoRNAs are further processed, generating short fragments with non-canonical functions. Generation of these processed snoRNAs (psnoRNAs) is not well understood; however, it has been suggested that they may arise from the same host intron and depend on stability and protein interactions (13). The nucleolar accumulation of *Snord116* snoRNAs coincides with increased transcription of the locus, an increase in nucleolar size during early postnatal development and chromatin decondensation of the paternally expressed *Snrpn-Ube3a* allele, detected by DNA FISH (10).

116HG is a long ncRNA (lncRNA) generated from the spliced exons of the *Snord116* primary transcript. *116HG* is retained within the nucleus and localizes to its paternally decondensed site of transcription, forming an 'RNA cloud', which associates with the *Snord116* locus as well as other genes with epigenetic, metabolic and circadian functions regulating their expression in a time-of-day-dependent manner (11). The *116HG* cloud is significantly larger during light hours, corresponding to the downregulated expression of its gene targets during sleep (14). Colocalized nuclear accumulation of the unspliced transcript and the spliced *116HG* indicate that splicing occurs locally at the site of paternal expression (11). Although splicing is required for *116HG* formation and *Snord116* snoRNA biogenesis, the mechanism of this process and its specificity for neurons is not well understood.

In an effort to determine phenotypes associated with genes within the PWS region, mouse models carrying deletions of nearly every paternally expressed gene in the human 15q11-q13 locus, either individually or as part of a large deletion, have been created and characterized (15). Although some models exhibit a subset of PWS-like phenotypes, issues of lethality complicate phenotypic analyses of adult mice in some models, and no current mouse model of PWS exhibits consistency in the late onset obesity characteristic of PWS (15–17). Currently, two mouse models ($PWScr^{m+/p-}$ and $Snord116^{+/-}$) carry deletions of the minimal *Snord116* PWS critical region, and display postnatal growth deficiency characteristic of the early failure to thrive phenotype exhibited by PWS patients as well as some hyperphagic behavior (18,19). Activation of maternal *Snord116* expression rescued the growth retardation and postnatal lethality phenotypes of the $PWScr^{m+/p-}$ small deletion model, supporting *Snord116* as the PWS-critical region (20). Although the snoRNAs have previously been the main focus of studies of the *Snord116* locus, transgenic expression of a single copy of *Snord116* snoRNA failed to rescue the phenotype of a *Snrpn-Ube3a* deletion mouse model, suggesting either that the *Snord116* functional unit is not restricted solely to the snoRNAs or that multiple copies are required (19,21). Reintroduction of multiple copies of *Snord116* snoRNAs expressed from the introns of another host gene failed to rescue the growth retardation phenotype of $PWScr^{m+/p-}$ mice, highlighting the functional significance of the *116HG* (20). Importantly, the regulation of circadian and metabolic gene expression by *116HG* leads to dysregulated energy expenditure in mice deficient for paternal *Snord116*, suggesting that the lncRNA *116HG* may play a role in the pathogenesis of PWS (14). Finally, the introns of the *Snord116* primary transcript may play a role in the regulation of *Ube3a-ats* progression by regulating chromatin compaction

through the formation of R-loops (22). These studies have illustrated the genetic complexity of the *Snord116* locus and the potential functional capacity of multiple elements within this lncRNA.

We designed a novel transgenic *Snord116* mouse to characterize the processing and formation of these *Snord116* RNA products, and define the mechanism regulating the brain specificity of these processes. By driving expression of *Snord116* with a ubiquitous promoter, we investigated the requirements for *Snord116* processing in multiple tissues and the potential of our transgene to compensate for the molecular deficits observed in *Snord116*$^{+/-}$ mice. We show that *Snord116* expression is not sufficient for the production of snoRNAs or the *116HG*, and that the formation of these products is blocked at the level of tissue-specific splicing. Our data demonstrate a requirement for *Rbfox3* in the neuron-specific splicing of *Snord116*, and an active paternal *Snord116* allele in the localization of its processed RNA components, providing a better understanding of the requirements of *Snord116* function in the development of potential future therapies for PWS.

Results

Transgenic *Snord116* integrates into the genome and is expressed in many tissues

To reintroduce *Snord116* in a highly expressed, ubiquitous manner to paternally *Snord116*-deficient mice, we engineered a novel 'complete' *Snord116* transgene (Ctg) containing three complete *Snord116* repeats under the control of a cytomegalovirus (CMV) promoter (Fig. 2A). Each unit of the *Snord116* repeat contained an intronically encoded snoRNA flanked by *116HG* exons, as organized in the genomic DNA. This construct was randomly inserted into the genome by pronuclear injection of fertilized oocytes to create a transgenic mouse carrying nine copies of the construct, representing 27 copies of the *Snord116*

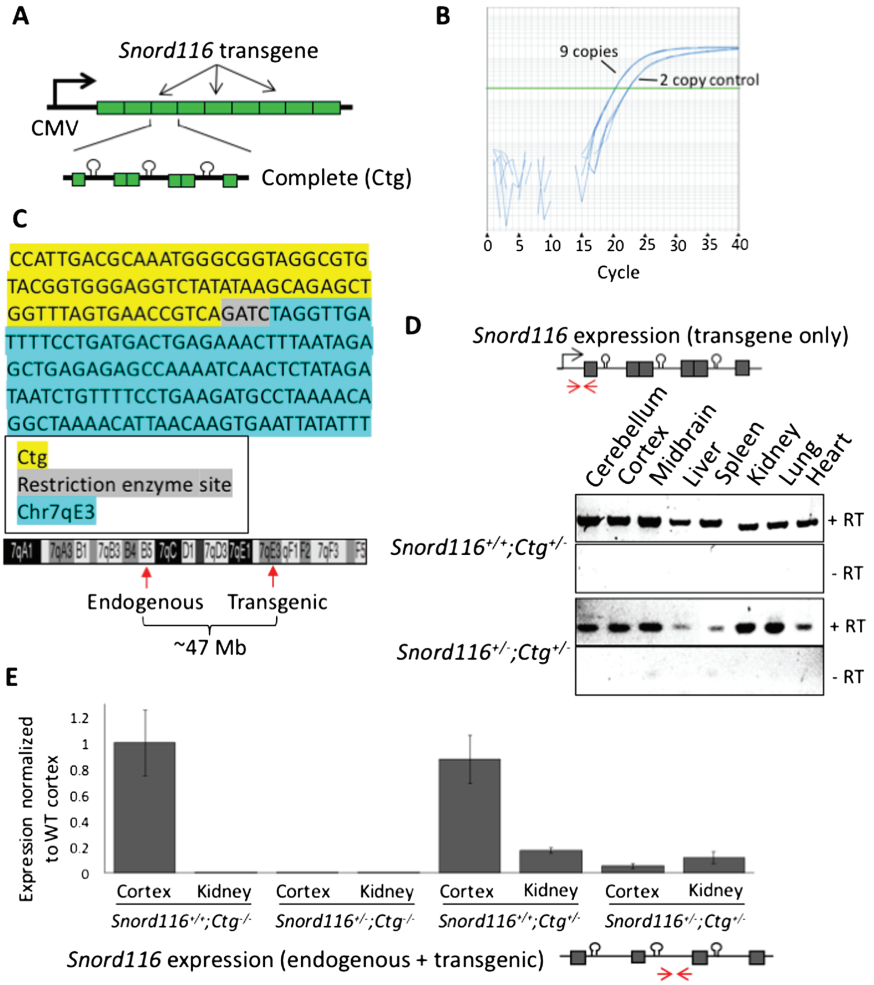

Figure 2. The *Snord116* transgene contains 27 copies of the *Snord116* repeat unit and is ubiquitously expressed. (**A**) Schematic of the *Snord116* transgene construct design containing nine copies of the 3-copy *Snord116* repeat unit (Ctg). (**B**) Copy number analysis indicates insertion of the *Snord116* transgene nine times in *Snord116*$^{+/+}$;*Ctg*$^{+/-}$ transgenic mice. (**C**) The location of *Snord116* transgene insertion was identified at chromosome 7qE3 by inverse PCR. The sequence amplified at the ligation between the 5′ end of the transgene and its site of insertion mapped to chromosome 7 is shown. Diagram of chromosome 7 indicating the locations of the endogenous and transgenic loci ~47 Mb apart. (**D**) The *Snord116* transgene shows ubiquitous expression in all tissues tested using transgene-specific primers on both WT and *Snord116*$^{+/-}$ backgrounds. The locations of the transgene-specific primers are shown as red arrows in the construct diagram. (**E**) Quantification of combined endogenous and transgenic *Snord116* primary transcript expression for all genotypes in cortex and kidney indicates the relative contribution of the *Snord116* transgene both in the presence and absence of endogenous *Snord116*. Primer locations are shown as red arrows in the transcript diagram. Statistical significance testing by analysis of variance (ANOVA) with Tukey correction is provided in Supplementary Table 1.

repeat unit (Fig. 2B). Mice were tested for transgene insertion by polymerase chain reaction (PCR) using primers specific to the transgene and inverse PCR was performed to identify the genomic location of the transgene integration at 7qE3, approximately 47 Mb from the endogenous *Snord116* locus (Fig. 2C). This falls outside of the 15q11-q13 imprinted locus and is therefore not expected to be co-regulated with endogenous *Snord116*. Transgenic *Snord116* insertion overlaps with the poorly characterized gene *Gm1966*, which has been reported as both an unprocessed pseudogene as well as a protein-coding gene in different databases. Overall, no anatomical differences were observed between the brains of the wild-type and transgenic mice.

The *Snord116*$^{+/-}$ PWS mouse model carries a ~150 kb deletion of *Snord116*, representing the smallest region of overlap for human PWS deletions (6,7,9,19). *Snord116*$^{+/-}$ mice recapitulate the neonatal failure to thrive exhibited by PWS patients and exhibit altered energy expenditure (14,19). We crossed *Snord116*$^{+/+}$;*Ctg*$^{+/-}$ transgenic females to *Snord116*$^{+/-}$ males to produce mice deficient for endogenous paternal *Snord116* but carrying the transgene (*Snord116*$^{+/-}$;*Ctg*$^{+/-}$) and littermate controls (*Snord116*$^{+/+}$;*Ctg*$^{+/-}$, *Snord116*$^{+/+}$;*Ctg*$^{-/-}$ and *Snord116*$^{+/-}$;*Ctg*$^{-/-}$). To ensure that the *Snord116* transgene was not transcriptionally silenced, we tested the expression of the transgene in both WT (*Snord116*$^{+/+}$;*Ctg*$^{+/-}$) and PWS (*Snord116*$^{+/-}$;*Ctg*$^{+/-}$) backgrounds, confirming expression in several tissues, including those in which *Snord116* is not endogenously expressed (12) (Fig. 2D). Quantification of combined endogenous and transgenic *Snord116* expression indicates that the expression levels of the transgenic primary transcript may be impacted by its chromosomal context and processing (Fig. 2E, Supplementary Material, Table S1).

Transgenic *Snord116* snoRNAs localize with endogenous snoRNAs specifically in neuronal nucleoli in wild-type but not *Snord116*$^{+/-}$ mice

Endogenous *Snord116* expression is restricted to neurons in mice; however, we sought to determine if transgenic *Snord116* was sufficient to recruit the required processing factors for the generation of functional snoRNAs. The ubiquitous expression pattern of the *Snord116* transgene allowed us to examine the processing and localization of *Snord116* snoRNAs outside of the neuronal lineage. We examined *Snord116* snoRNA localization by RNA FISH in coronal brain sections using probes that detect both the endogenous and transgenic *Snord116* RNAs (Fig. 3A, Supplementary Material, Figs S1 and 2). Despite ubiquitous expression of the *Snord116* transcript in multiple tissues, detection of snoRNA nucleolar localization was limited to neurons in the brain, as it was not observed in non-neuronal nuclei. *Snord116* snoRNAs were clearly detected in WT nucleoli of Purkinje neurons in the cerebellum and localized to the single large nucleolus, which we have previously characterized by α-nucleolin staining (10). As expected, snoRNAs were not observed in *Snord116*$^{+/-}$ neurons due to the lack of paternal *Snord116* expression. In *Snord116*$^{+/+}$;*Ctg*$^{+/-}$ mice, the intensity of the nucleolar snoRNA RNA FISH signal was significantly greater than in WT nucleoli (*Snord116*$^{+/+}$;*Ctg*$^{-/-}$) (Fig. 3B), indicating that transgenic *Snord116* potentially contributes to increasing the snoRNA population. SnoRNAs were also detected in the cortex of *Snord116*$^{+/+}$;*Ctg*$^{-/-}$ and *Snord116*$^{+/+}$;*Ctg*$^{+/-}$ mice. However, in the absence of endogenous *Snord116* (*Snord116*$^{+/-}$;*Ctg*$^{+/-}$), expression of the transgene was not sufficient to produce detectable snoRNA accumulation

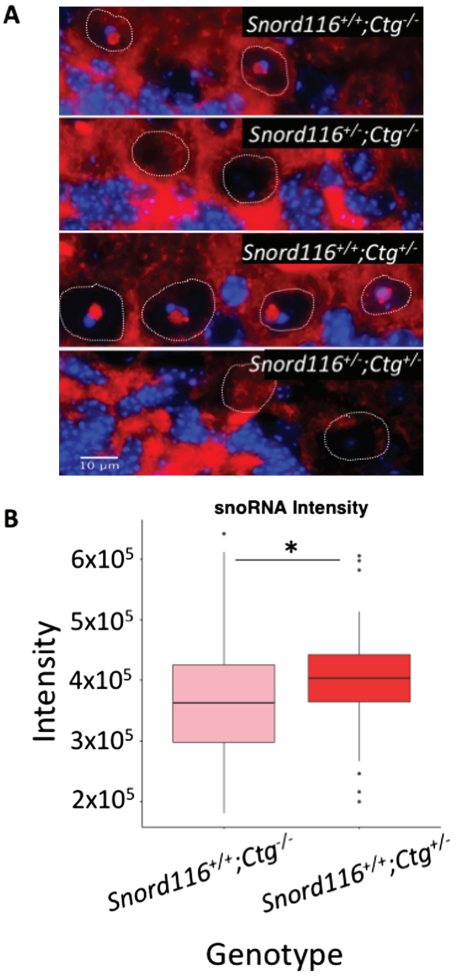

Figure 3. Transgenic *Snord116* colocalizes with endogenous *Snord116*, but does not localize to nucleoli in neurons lacking endogenous *Snord116* expression. (**A**) RNA FISH for *Snord116* snoRNAs in Purkinje neurons. Nuclei are stained with DAPI (blue) and the boundaries of Purkinje nuclei are denoted by white dotted lines. *Snord116* snoRNAs are shown in red localized within nucleoli of Purkinje neurons. (**B**) Quantification of RNA FISH signal shows significantly stronger *Snord116* snoRNA signal in *Snord116*$^{+/+}$;*Ctg*$^{+/-}$ Purkinje nucleoli compared to *Snord116*$^{+/+}$;*Ctg*$^{-/-}$. *$P = 0.006$ by *t*-test.

within neuronal nucleoli in any brain region or in non-neuronal tissues (Supplementary Material, Figs. S1 and 2). These results indicate that although transgenic *Snord116* is able to contribute to endogenous snoRNAs, transcription of the primary transcript is not sufficient for the processing or localization of these RNAs in non-neuronal and *Snord116*-deficient neuronal tissues.

Neuron-specific splicing of transgenic *Snord116* requires *Rbfox3*/NeuN

The discrepancy between expression of the primary transcript and production of functional snoRNA products from the *Snord116* transgene led us to determine if splicing was the limiting factor in snoRNA processing. Using transgene-specific primers, we assessed splicing of transgenic *Snord116* in several neuronal and non-neuronal tissues of *Snord116*$^{+/+}$;*Ctg*$^{+/-}$ and *Snord116*$^{+/-}$;*Ctg*$^{+/-}$ mice. Reverse transcription-PCR (RT-PCR) analysis demonstrated that splicing of transgenic *Snord116* was restricted to neuronal tissues of both *Snord116*$^{+/+}$;*Ctg*$^{+/-}$and

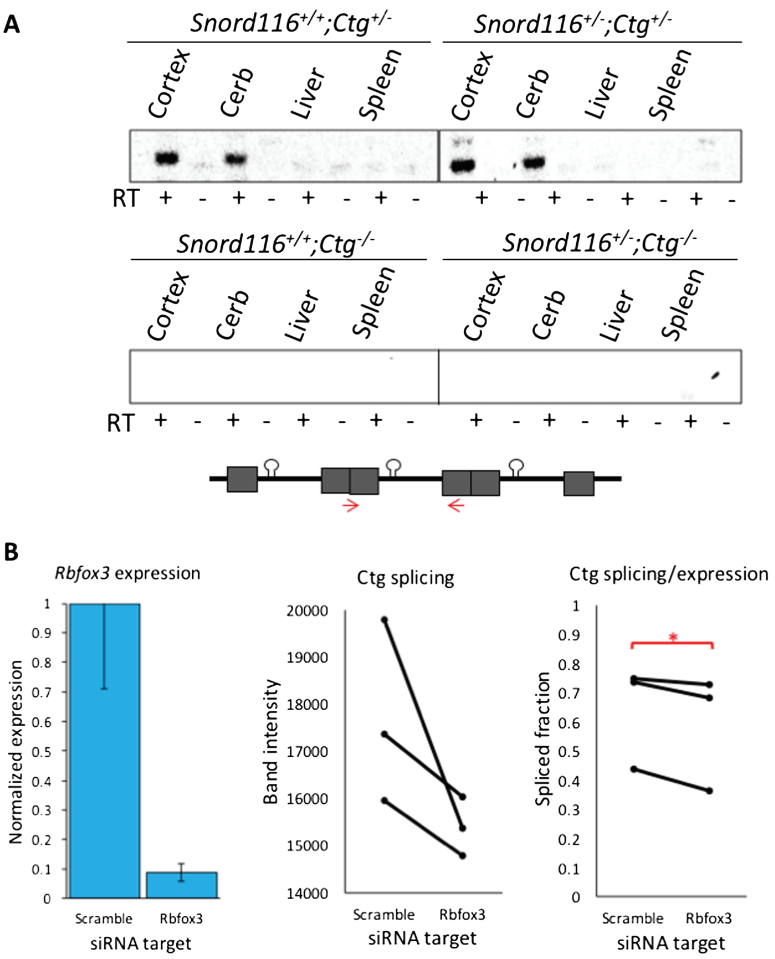

Figure 4. Splicing of transgenic *Snord116* is restricted to neuronal tissues and is reduced by *Rbfox3* knockdown. (**A**) Splicing of transgenic *Snord116* is unique to neuronal tissues in both *Snord116*$^{+/+}$;*Ctg*$^{+/-}$ and *Snord116*$^{+/-}$;*Ctg*$^{+/-}$ mice. Bands indicate the spliced product of the Ctg transgene. RT (–) lanes indicate negative reverse transcriptase controls. The locations of splice primers are shown as red arrows in the construct diagram. (**B**) Knockdown of *Rbfox3* expression in *Snord116*$^{+/-}$;*Ctg*$^{+/-}$ NPC-derived neurons reduces splicing of *Snord116*. *Rbfox3* levels are shown in the left panel, normalized to Gapdh. Knockdown levels are graphed relative to levels detected in the negative scramble siRNA condition. Absolute intensity of the spliced Ctg is shown for each condition in the middle panel. The spliced fraction of the expressed transgene (splicing/expression) is significantly lower after *Rbfox3* knockdown compared to a scramble siRNA control (right panel). *$P < 0.05$ by paired *t*-test.

Snord116$^{+/-}$;*Ctg*$^{+/-}$mice (Fig. 4A) even though primary transcripts were detected in multiple tissue types (Fig. 2D). These results demonstrate that splicing may explain the tissue-specific differences between transcript expression and snoRNA localization, but not the deficiency of snoRNA processing in neurons of *Snord116*$^{+/-}$;*Ctg*$^{+/-}$ mice.

NeuN is commonly used in immunofluorescence staining as a neuron-specific marker, and has now been identified as the neuron-specific splicing factor, *Rbfox3* (23). To test the hypothesis that *Rbfox3*/NeuN regulates neuron-specific splicing of the *Snord116* transgene, we performed an siRNA knockdown of *Rbfox3* in neurons derived from *Snord116*$^{+/-}$;*Ctg*$^{+/-}$ neural progenitor cells (NPCs), reducing *Rbfox3* expression to about 9% of levels detected in scramble siRNA-treated NPCs (Fig. 4B and Supplementary Material, Fig. S3). The expression of the transgenic *Snord116* primary transcript was unaffected following *Rbfox3* siRNA knockdown; however, the proportion of the primary transcript that was spliced (splicing/expression) was significantly reduced (Fig. 4B and Supplementary Material, Fig. S3). To further examine a role for Rbfox3 in *Snord116* splicing, we utilized a published dataset of RNA sequencing from *Rbfox3* knockout mouse cerebral cortex (24). Visualization of exon junctions within the *Snord116* locus by sashimi plot using the Integrative Genomics Viewer (IGV) browser demonstrated that loss of Rbfox3 leads to pronounced dysregulation of exon splicing between *Snord116* and *Ube3a* (Supplementary Material, Fig. S4). Together, these results demonstrate that *Rbfox3* levels affect neuronal *Snord116* splicing, and suggest that *Rbfox3*/NeuN is essential for the processing of intron-embedded snoRNAs.

The transgenic host gene *116HG* RNA cloud localizes to the endogenous, but not the transgenic *Snord116* locus, only in wild-type neurons

In addition to the nucleolar snoRNAs, the spliced exons of the *Snord116* locus are retained as an RNA cloud that localizes to the site of transcription on the active paternal allele in wild-type neurons (22) (Fig. 1). We therefore asked whether the transgenically-encoded *116HG* localized to its own site of transcription using RNA FISH with a probe designed to detect the spliced junctions of both endogenous and transgenic *116HG*. Similarly to the *Snord116* snoRNA localization, *116HG* FISH signals were observed as a single nuclear cloud in both *Snord116*$^{+/+}$;*Ctg*$^{-/-}$ and *Snord116*$^{+/+}$;*Ctg*$^{+/-}$ neurons, but not *Snord116*$^{+/-}$;*Ctg*$^{-/-}$ or *Snord116*$^{+/-}$;*Ctg*$^{+/-}$ neurons (Fig. 5A and

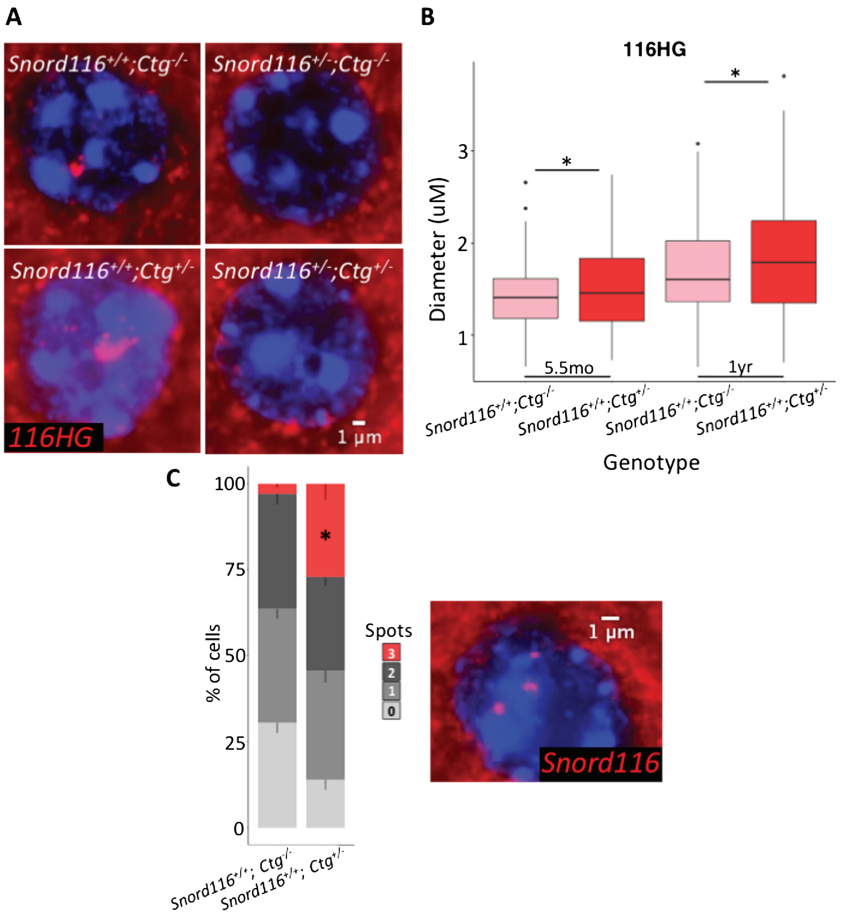

Figure 5. Transgenic *116HG* colocalizes with the endogenous *116HG* RNA cloud, but is not detected in the nuclei of neurons lacking endogenous *Snord116* expression. (**A**) RNA FISH for *116HG* in a cortical neuronal nucleus. Nuclei are stained with DAPI (blue) and the *116HG* RNA FISH signal is shown in red. (**B**) Quantification of RNA FISH signal shows a single significantly larger *116HG* RNA cloud in *Snord116*$^{+/+}$;*Ctg*$^{+/-}$ neuronal nuclei compared to *Snord116*$^{+/+}$;*Ctg*$^{-/-}$. *T*-test, $P = 0.002$. (**C**) DNA FISH of *Snord116* in neuronal nuclei shows three detectable *Snord116* loci (red) in a significant proportion of *Snord116*$^{+/+}$;*Ctg*$^{+/-}$ neuronal nuclei (blue), indicating a lack of colocalization. *$P < 0.0001$ by *t*-test.

Figs. S5 and 6). In mice of two different ages (5.5 months and 1 year), the single *116HG* RNA FISH signal was significantly larger in *Snord116*$^{+/+}$;*Ctg*$^{+/-}$ compared to *Snord116*$^{+/+}$;*Ctg*$^{-/-}$ neurons (Fig. 5B), suggesting that the transgenic spliced *116HG* localized and contributed to the *116HG* RNA cloud on the endogenous paternal allele. By DNA FISH, distinct nuclear locations of the three alleles (endogenous maternal and paternal, plus transgene) were observed (Fig. 5C), demonstrating the absence of colocalization of the transgenic allele with the active paternal allele at the chromosomal level. In addition to our molecular analysis, we measured body weight for all genotypes from weaning until postnatal week 11. It has previously been reported that *Snord116*$^{+/-}$ mice weigh significantly less than their WT littermates within this time frame (14,19), therefore we sought to determine whether the *Snord116* transgene would rescue the deletion phenotype. Concordant with the lack of *Snord116* molecular rescue of the *116HG* RNA cloud and the *Snord116* snoRNAs, *Snord116*$^{+/-}$;*Ctg*$^{+/-}$ mice had a significantly lower body weight than *Snord116*$^{+/+}$;*Ctg*$^{-/-}$ mice, similar to the weights observed in *Snord116*$^{+/-}$;*Ctg*$^{-/-}$ mice (Fig. 6A and Supplementary Material, Table S2) (14). Interestingly, the additive effect of endogenous and transgenic *Snord116* (*Snord116*$^{+/+}$;*Ctg*$^{+/-}$) also resulted in decreased body weight compared to expression of the endogenous locus alone (*Snord116*$^{+/+}$;*Ctg*$^{-/-}$), reaching significance at postnatal week 11, suggesting that expression in tissues outside of the brain as in *Snord116*$^{+/+}$;*Ctg*$^{+/-}$ and *Snord116*$^{+/-}$;*Ctg*$^{+/-}$ mice may have a significant impact on metabolism.

To test the hypothesis that a second requirement for *116HG* complementation is an active endogenous *Snord116* locus, we utilized another transgenic mouse model, in which the maternal mouse PWS-IC has been replaced by the human PWS-IC (PWS-IC^{Hs}/+) (25). Because the human PWS-IC does not become imprinted in mice, the normally silent maternal allele undergoes chromatin decondensation and expresses *Snrpn*, snoRNAs and *Ube3a-ats* in neurons, similar to the paternal allele (Fig. 6B) (10). In neuronal nuclei of PWS-IC^{Hs}/+ mice, two distinct *116HG* RNA clouds were observed by RNA FISH, demonstrating that the requirement for *116HG* RNA localization is an active endogenous *Snord116* allele, not simply transcription of *Snord116*. Together, these results demonstrate that complementation by transgenic *Snord116* requires additional factors both *in trans* (*Rbfox3*/NeuN) and *in cis* (chromatin decondensation).

Discussion

This study utilized a novel 27-copy *Snord116* transgenic mouse to characterize the requirements for *Snord116* processing and assess the molecular functional capacity of transgenic *Snord116* in the absence of endogenous paternal expression. We demon-

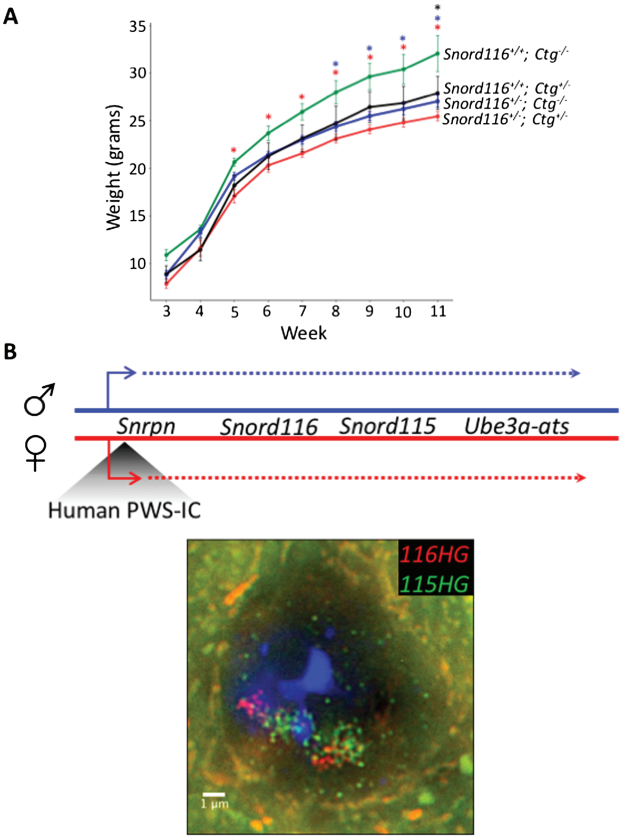

Figure 6. Transgenic *Snord116* does not rescue the weight phenotype observed in *Snord116*$^{+/-}$ mice. (**A**) Weight curves of all genotypes from *Snord116*$^{+/-}$;*Ctg*$^{-/-}$ X *Snord116*$^{+/+}$;*Ctg*$^{+/-}$ cross. Mice carrying the *Snord116* transgene, either on a WT or *Snord116*$^{+/-}$ background weigh significantly less than WT mice, and are phenotypically more similar to *Snord116*$^{+/-}$ mice. N = 4 *Snord116*$^{+/+}$;*Ctg*$^{-/-}$ (WT), 4 *Snord116*$^{+/+}$;*Ctg*$^{+/-}$ (Ctg/WT), 13 *Snord116*$^{+/-}$;*Ctg*$^{-/-}$ (Prad), 13 *Snord116*$^{+/-}$;*Ctg*$^{+/-}$ (Ctg/Prad). *$P < 0.05$ by repeated measures ANOVA, Benjamini–Hochberg post-hoc correction (results in Supplementary Material, Table S2). (**B**) Map of the 15q11-q13 locus in PWS-IC^{Hs}/+ mice with the paternal allele indicated in blue and the maternal allele indicated in red. RNA FISH for *116HG* (red) and *115HG* (green) in a PWS-IC^{Hs}/+ neuronal nucleus, with two decondensed alleles, shows the formation of two distinct RNA clouds for each cluster, indicating the requirement for a decondensed endogenous locus for the localization of the spliced *116HG*.

strated that transgenic *Snord116* colocalizes with endogenous *Snord116* snoRNAs and *116HG* in the brain; however, transgenic *Snord116* expression alone is not sufficient for the formation of functional RNAs from this locus, as they are not detected in tissues outside of the brain. Additionally, trafficking of transgenic RNAs is impaired in the absence of endogenous paternal *Snord116*; therefore, nuclear RNA cloud formation is observed only in the presence of endogenous *Snord116* expression. Further, splicing of the *Snord116* transgene was restricted to the brain, despite expression in many tissues. This process is partially blocked by the knockdown of *Rbfox3* in NPC-derived neurons, suggesting a role for this neuron-specific splicing factor in the processing of *Snord116*. The introduction of transgenic *Snord116* also fails to rescue the weight phenotype observed in *Snord116*$^{+/-}$ mice.

Splicing represents a critical step in the regulation of gene expression in all tissues; however, the brain exhibits the highest levels of tissue-specific alternative splicing (26–28). Such tissue-specific splicing reflects the intricate cellular connections and functional diversity within the brain and exemplifies the complex expression and regulatory networks observed in the brain and during development. Brain-specific splicing factors provide an important mechanism for the co- and post-transcriptional regulation involved in processes such as neurogenesis and synapse formation through the spatiotemporal control of RNA expression, processing and localization (29,30). The Rbfox family of splicing factors is important in the regulation of brain development, with *Rbfox3* expression uniquely confined to mature postmitotic neurons (31). Neuronal co-expression and the presence of the (U)GCAUG-binding motif (32,33) within the introns of the *Snord116* transcript support the role for *Rbfox3* in the processing of *Snord116* in the brain. In addition, a recent study modeling the *Rbfox3* regulatory network by crosslinking and immunoprecipitation followed by high-throughput sequencing identified significant peaks within the introns of *Ipw*, validating our *Snord116*-specific analysis of *Rbfox3* activity (33). Interestingly, *RBFOX3* has been shown to be expressed at low levels in some immortalized human cell lines, where levels may be sufficient for the production of *SNORD116* RNA products, or may be compensated for by the expression of other splicing factors including *RBFOX1* or *RBFOX2*.

Ube3a, another gene within the 15q11-q13 locus, is paternally imprinted in neurons, in which the paternal expression of the *Snrpn-Ube3a* transcript extends through the anti-sense to *Ube3a*, blocking transcription of paternal *Ube3a* and leading to maternal-specific expression (34–36). Interestingly, in *Rbfox3*/NeuN-negative cells of the suprachiasmatic nucleus (SCN), paternal *Ube3a* expression is observed (37). Due to its high level of GC skew, transcription through *Snord116* results in the formation of *R*-loops, modulating the balance between chromatin state and transcription elongation. Stabilization of these *R*-loops by topotecan treatment stalls RNA polymerase II progression, blocking transcription through *Ube3a-ats* and resulting in biallelic *Ube3a* expression (22). Conversely, a study of genome stability demonstrated the ability of the ASF/SF2 splicing factor to interact with *R*-loops, repressing their formation through interaction with the nascent RNA (38). The *Rbfox3*-dependent silencing of paternal *Ube3a* in the SCN suggests that neuron-specific splicing of *Snord116* by *Rbfox3* may be important for maintaining the balance of *R*-loop formation, promoting transcription through *Ube3a-ats* and paternal imprinting of *Ube3a* in neurons.

It is important to note that the chromatin context of the transgene likely contributes to differences in the expression and processing of the primary transcript, which are lower than WT levels. It is therefore possible that the level of *Snord116* expression produced by the transgene alone in *Snord116*$^{+/-}$;*Ctg*$^{+/-}$ mice may not be sufficient to compensate for the loss of endogenous *Snord116*. Despite low levels of transgenic primary transcript however, in the presence of splicing by *Rbfox3* and the endogenous chromatin for localization, this transgenic primary transcript contributes significantly to the formation of mature RNA products in the brain. This indicates a potential multi-level deficit in the production of functional RNAs from transgenic *Snord116* in *Snord116*$^{+/-}$;*Ctg*$^{+/-}$ neurons and in all non-neuronal tissues. Paternal *Snord116* is GC skewed, resulting in *R*-loop formation, histone displacement and chromatin decondensation upon neuronal transcription and the specific localization of the *116HG* to its site of transcription at the decondensed paternal allele suggests a chromatin-state-dependent accumulation of *116HG* (22). The formation of two *116HG* RNA clouds in PWS-IC^{Hs}/+ neuronal nuclei demonstrates the requirement for a decondensed endogenous allele for the localization of *Snord116*, suggesting that chromatin decondensation may

mediate RNA–DNA interactions necessary to anchor the *116HG* to its proper subnuclear domain. The lack of phenotypic rescue by the *Snord116* transgene is in agreement with the lack of rescue at the molecular level; however, the negative combinatorial effect of endogenous and transgenic *Snord116* may reflect the aberrant expression of *Snord116* in tissues outside of the brain important for metabolism. Further study of the mechanisms of *Snord116* localization would benefit our understanding of the requirements for *Snord116* function and enable the development of more effective therapies in the future.

Materials and Methods

Mouse husbandry

C57BL/6J (WT) and B6(Cg)-Snord116tm1.1Uta/J (*Snord116*$^{+/-}$) mice were obtained from Jackson Laboratory (Bar Harbor, ME, USA). *Ctg*$^{+/-}$ mice were generated by the Mouse Biology Program (UC Davis). All mice were housed in a 12 h light:12 h dark temperature-controlled room and fed a standard diet of PicoLab mouse chow 20 (PMI International, St Louis, MO, USA). Heterozygous deletion male mice (*Snord116*$^{+/-}$) were bred with heterozygous *Ctg* transgenic females (*Ctg*$^{+/-}$) to generate littermates of each of the following genotypes: *Snord116*$^{+/+}$;*Ctg*$^{-/-}$ (WT), *Snord116*$^{+/-}$;*Ctg*$^{-/-}$ (Prad), *Snord116*$^{+/+}$;*Ctg*$^{+/-}$ (Ctg/WT), *Snord116*$^{+/-}$;*Ctg*$^{+/-}$ (Ctg/Prad). All mice used for this study were male and tissues were collected during light hours (ZT0-ZT12).

RNA FISH and DNA FISH

Snord116 BAC RP23-358G20 was ordered from BACPAC Resources (Children's Hospital Oakland Research Institute). Nick translation of DIG-labeled probes and DNA FISH was performed as described previously (10). RNA FISH was performed as described previously (10).

116HG probes = AATGCAACCCTTTTAACTCAG (Exiqon), pooled probes (Agilent).

snoRNA probe = TTCCGATGAGAGTGGCGGTACAGA (Exiqon).

Microscopy

Slides were imaged on an Axioplan 2 fluorescence microscope (Carl Zeiss, Inc., NY, USA), equipped with a Qimaging Retiga EXi high-speed uncooled digital camera and analyzed using iVision Software (BioVision Technologies, Inc., Exton, PA, USA). Images were captured using a 100× oil objective and 1× camera zoom. *116HG* RNA cloud measurements were taken as two perpendicular cross sections through the center of the RNA cloud and averaged for RNA cloud size. snoRNA intensity was measured as the sum of the intensity of each pixel divided by the area measured. All measurements were converted from pixel counts to microns according to objective and zoom (1px = 0.069 μm). All measurements and spot counting were blinded to minimize bias.

Reverse transcriptase PCR (RT-PCR) and quantitative RT-PCR (qRT-PCR)

RNA was isolated with the RNeasy mini kit (Qiagen, Hilden, Germany) and complementary DNA (cDNA) was synthesized using the QuantiTect Reverse Transcription Kit (Qiagen). For qRT-PCR, cDNA was amplified using the SensiFAST SYBR Lo-Rox Kit (Bioline, London, UK). Custom primers were designed using Primer3 software.

Ctg expression (transgene specific):

F – taagcagagctggtttagtgaacc; R – aacagttcgatggagactcagttgg

Ctg splicing (transgene specific):

F – cctgagttaaaaggcggccg; R – gccatttcctctgcatgttt

Rbfox3 expression:

F – aatttttcccgaattgcccgaac; R – atgaagcagcacagacagacaa

Snord116 expression (endogenous + transgenic):

F – atgcaggctgctggtagagt; R – cctccaaggcttagctcctt

Gapdh expression (39):

F – caaggagtaagaaaccctggacc; R – cgagttgggatagggcctct

NPC and neuron culture

Embryos were dissected and cortices removed at E15. NPCs were isolated as described previously (40) and cultured in NEP Complete media supplemented with GlutaMAX. To differentiate, neurospheres were dissociated with Accutase (Invitrogen) and filtered for a single-cell suspension. Plates were coated with Poly-D-lysine (Sigma, St. Louis, MO, USA) and laminin (Invitrogen) and media was changed to Neurobasal with retinoic acid and brain-derived neurotrophic factor.

siRNA knockdown

Rbfox3 was knocked down using a pool of three Stealth RNAi siRNA or a negative control siRNA at 55 pmol RNAi per 60 mm dish (Life Technologies, Carlsbad, CA, USA). Neurons were differentiated for 7 days followed by 3 days of knockdown. RNA was then extracted and evaluated for knockdown efficiency by qRT-PCR and expression/splicing by RT-PCR.

Inverse PCR

Genomic DNA was isolated from tail clipping using the Gentra Puregene Kit (Qiagen). DNA was digested with DpnII and circularized by T4 ligation (Promega, Madison, WI, USA). Primers were designed to the known transgene sequence to amplify the unknown flanking genomic region. The PCR product was gel purified and sequenced by Sanger sequencing. Sequences flanking the DpnII restriction site were mapped to the transgene and the genome flanking.

Inverse PCR primers:

F – gatttccaagtctccaccccat; R – ggctatgaactaatgaccccgt

RNA-sequencing analysis

SRA files were downloaded from GEO (GSE84786) (24) and converted to fastq files using fastq-dump, splitting files for paired-end reads. Reads were trimmed for adapters and quality using the following parameters: ILLUMINACLIP:TruSeq3-PE.fa:2:30:10:8:T LEADING:15 TRAILING:15 SLIDINGWINDOW:

4:15. An insert size of 200 bp was used based on Picard metrics and reads were aligned to mm10 using TopHat2. Bam index files were built using Picard Tools and stranded bed files were created and used to create bedGraph and bigwig files for visualization as custom tracks on the UCSC genome browser. Raw bam files were loaded into the IGV browser to create sashimi plots (MISO framework) (41,42).

Supplementary Material

Supplementary Material is available at *HMG* online.

Conflict of Interest statement. None declared.

Funding

National Institute of Health (R01 NS076263, R56 NS076263-06 to J.M.L., T32 GM007377 to R.L.C.); Intellectual and Developmental Disabilities Research Center (U54 HD079125) and the Foundation for Prader–Willi Research.

References

1. Cassidy, S.B., Schwartz, S., Miller, J.L. and Driscoll, D.J. (2012) Prader–Willi syndrome. *Genet. Med.*, **14**, 1–10.
2. Runte, M., Hüttenhofer, A., Groß, S., Kiefmann, M., Horsthemke, B. and Buiting, K. (2001) The IC-SNURF–SNRPN transcript serves as a host for multiple small nucleolar RNA species and as an antisense RNA for UBE3A. *Hum. Mol. Genet.*, **10**, 2687–2700.
3. Landers, M., Bancescu, D.L., Le Meur, E., Rougeulle, C., Glatt-Deeley, H., Brannan, C., Muscatelli, F. and Lalande, M. (2004) Regulation of the large (~1000 kb) imprinted murine Ube3a antisense transcript by alternative exons upstream of Snurf/Snrpn. *Nucleic Acids Res.*, **32**, 3480–3492.
4. Sutcliffe, J.S., Nakao, M., Christian, S., Orstavik, K.H., Tommerup, N., Ledbetter, D.H. and Beaudet, A.L. (1994) Deletions of a differentially methylated CpG island at the SNRPN gene define a putative imprinting control region. *Nat. Genet.*, **8**, 52–58.
5. Buiting, K., Saitoh, S., Gross, S., Dittrich, B., Schwartz, S., Nicholls, R.D. and Horsthemke, B. (1995) Inherited microdeletions in the Angelman and Prader–Willi syndromes define an imprinting centre on human chromosome 15. *Nat. Genet.*, **9**, 395–400.
6. Duker, A.L., Ballif, B.C., Bawle, E.V., Person, R.E., Mahadevan, S., Alliman, S., Thompson, R., Traylor, R., Bejjani, B.A., Shaffer, L.G. *et al.* (2010) Paternally inherited microdeletion at 15q11.2 confirms a significant role for the SNORD116 C/D box snoRNA cluster in Prader–Willi syndrome. *Eur. J. Hum. Genet.*, **18**, 1196–1201.
7. de Smith, A.J., Purmann, C., Walters, R.G., Ellis, R.J., Holder, S.E., Van Haelst, M.M., Brady, A.F., Fairbrother, U.L., Dattani, M., Keogh, J.M. *et al.* (2009) A deletion of the HBII-85 class of small nucleolar RNAs (snoRNAs) is associated with hyperphagia, obesity and hypogonadism. *Hum. Mol. Genet.*, **18**, 3257–3265.
8. Sahoo, T., Del Gaudio, D., German, J.R., Shinawi, M., Peters, S.U., Person, R.E., Garnica, A., Cheung, S.W. and Beaudet, A.L. (2008) Prader–Willi phenotype caused by paternal deficiency for the HBII-85 C/D box small nucleolar RNA cluster. *Nat. Genet.*, **40**, 719–721.
9. Bieth, E., Eddiry, S., Gaston, V., Lorenzini, F., Buffet, A., Auriol, F.C., Molinas, C., Cailley, D., Rooryck, C., Arveiler, B. *et al.* (2014) Highly restricted deletion of the SNORD116 region is implicated in Prader–Willi Syndrome. *Eur. J. Hum. Genet.*, **23**, 252–255.
10. Leung, K.N., Vallero, R.O., Dubose, A.J., Resnick, J.L. and Lasalle, J.M. (2009) Imprinting regulates mammalian snoRNA-encoding chromatin decondensation and neuronal nucleolar size. *Hum. Mol. Genet.*, **18**, 4227–4238.
11. Vitali, P., Royo, H., Marty, V., Bortolin-Cavaille, M.-L. and Cavaille, J. (2010) Long nuclear-retained non-coding RNAs and allele-specific higher-order chromatin organization at imprinted snoRNA gene arrays. *J. Cell Sci.*, **123**, 70–83.
12. Cavaillé, J., Buiting, K., Kiefmann, M., Lalande, M., Brannan, C.I., Horsthemke, B., Bachellerie, J.P., Brosius, J. and Hüttenhofer, A. (2000) Identification of brain-specific and imprinted small nucleolar RNA genes exhibiting an unusual genomic organization. *Proc. Natl. Acad. Sci. U.S.A.*, **97**, 14311–14316.
13. Falaleeva, M. and Stamm, S. (2013) Processing of snoRNAs as a new source of regulatory non-coding RNAs: SnoRNA fragments form a new class of functional RNAs. *Bioessays*, **35**, 46–54.
14. Powell, W.T., Coulson, R.L., Crary, F.K., Wong, S.S., Ach, R.A., Tsang, P., Yamada, N.A., Yasui, D.H. and LaSalle, J.M. (2013) A Prader–Willi locus lncRNA cloud modulates diurnal genes and energy expenditure. *Hum. Mol. Genet.*, **22**, 4318–4328.
15. Bervini, S. and Herzog, H. (2013) Mouse models of Prader–Willi Syndrome: a systematic review. *Front. Neuroendocrinol.*, **34**, 107–119.
16. Purtell, L., Qi, Y., Campbell, L., Sainsbury, A. and Herzog, H. (2017) Adult-onset deletion of the Prader–Willi syndrome susceptibility gene Snord116 in mice results in reduced feeding and increased fat mass. *Transl. Pediatr.*, **6**, 88–97.
17. Polex-Wolf, J., Lam, B.Y.H., Larder, R., Tadross, J., Rimmington, D., Bosch, F., Jiménez Cenzano, V., Ayuso, E., Ma, M.K.L., Rainbow, K. *et al.* (2018) Hypothalamic loss of Snord116 recapitulates the hyperphagia of Prader–Willi syndrome. *J. Clin. Invest.*, **128**, 960–969.
18. Skryabin, B.V., Gubar, L.V., Seeger, B., Pfeiffer, J., Handel, S., Robeck, T., Karpova, E., Rozhdestvensky, T.S. and Brosius, J. (2007) Deletion of the MBII-85 snoRNA gene cluster in mice results in postnatal growth retardation. *PLoS Genet.*, **3**, e235.
19. Ding, F., Li, H.H., Zhang, S., Solomon, N.M., Camper, S.A., Cohen, P. and Francke, U. (2008) SnoRNA Snord116 (Pwcr1/MBll-85) deletion causes growth deficiency and hyperphagia in mice. *PLoS One*, **3**, e1709.
20. Rozhdestvensky, T.S., Robeck, T., Galiveti, C.R. and Raabe, C.A. (2016) Maternal transcription of non-protein coding RNAs from the PWS-critical region rescues growth retardation in mice. *Scientific Reports*, **6**, DOI: 10.1038/srep20398.
21. Tsai, T.F., Jiang, Y.H., Bressler, J., Armstrong, D. and Beaudet, A.L. (1999) Paternal deletion from Snrpn to Ube3a in the mouse causes hypotonia, growth retardation and partial lethality and provides evidence for a gene contributing to Prader–Willi syndrome. *Hum. Mol. Genet.*, **8**, 1357–1364.
22. Powell, W.T., Coulson, R.L., Gonzales, M.L., Crary, F.K., Wong, S.S., Adams, S., Ach, R.A., Tsang, P., Yamada, N.A., Yasui, D.H. *et al.* (2013) R-loop formation at Snord116 mediates topotecan inhibition of Ube3a-antisense and allele-specific chromatin decondensation. *Proc. Natl. Acad. Sci. U.S.A.*, **110**.

23. Kim, K.K., Adelstein, R.S. and Kawamoto, S. (2009) Identification of neuronal nuclei (NeuN) as Fox-3, a new member of the Fox-1 gene family of splicing factors. *J. Biol. Chem.*, **284**, 31052–31061.
24. Wang, H.-Y., Hsieh, P.-F., Huang, D.-F., Chin, P.-S., Chou, C.-H., Tung, C.-C., Chen, S.-Y., Lee, L.-J., Shur-Fen Gau, S. and Huang, H.-S. (2015) RBFOX3/NeuN is required for hippocampal circuit balance and function. *Scientific Reports*, **5**, DOI: 10.1038/srep17383.
25. Johnstone, K.A., DuBose, A.J., Futtner, C.R., Elmore, M.D., Brannan, C.I. and Resnick, J.L. (2006) A human imprinting centre demonstrates conserved acquisition but diverged maintenance of imprinting in a mouse model for Angelman syndrome imprinting defects. *Hum. Mol. Genet.*, **15**, 393–404.
26. de la Grange, P., Gratadou, L., Delord, M., Dutertre, M. and Auboeuf, D. (2010) Splicing factor and exon profiling across human tissues. *Nucleic Acids Res.*, **38**, 2825–2838.
27. Xu, Q., Modrek, B. and Lee, C. (2002) Genome-wide detection of tissue-specific alternative splicing in the human transcriptome. *Nucleic Acids Res.*, **30**, 3754–3766.
28. Yeo, G., Holste, D., Kreiman, G. and Burge, C.B. (2004) Variation in alternative splicing across human tissues. *Genome Biol.*, **5**, R74.
29. Zheng, S. and Black, D.L. (2014) Alternative pre-mRNA splicing in neurons: growing up and extending its reach. *Trends Genet*, **29**, 442–448.
30. Chih, B., Gollan, L. and Scheiffele, P. (2006) Alternative splicing controls selective trans-synaptic interactions of the neuroligin-neurexin complex. *Neuron*, **51**, 171–178.
31. Duan, W., Zhang, Y.-P., Hou, Z., Huang, C., Zhu, H., Zhang, C.-Q. and Yin, Q. (2015) Novel insights into NeuN: from neuronal marker to splicing regulator. *Mol. Neurobiol.*, **53**, 1637–1647.
32. Minovitsky, S., Gee, S.L., Schokrpur, S., Dubchak, I. and Conboy, J.G. (2005) The splicing regulatory element, UGCAUG, is phylogenetically and spatially conserved in introns that flank tissue-specific alternative exons. *Nucleic Acids Res.*, **33**, 714–724.
33. Weyn-vanhentenryck, S.M., Mele, A., Yan, Q., Sun, S., Farny, N., Zhang, Z., Xue, C., Herre, M., Silver, P.A. and Michael, Q. (2014) HITS-CLIP and integrative modeling define the Rbfox splicing-regulatory network linked to brain development and autism. *Cell Rep.*, **6**, 1139–1152.
34. Rougeulle, C., Cardoso, C., Fontes, M., Colleaux, L. and Lalande, M. (1998) An imprinted antisense RNA overlaps UBE3A and a second maternally expressed transcript. *Nat. Genet.*, **19**, 15–16.
35. Meng, L., Person, R.E. and Beaudet, A.L. (2012) Ube3a-ATS is an atypical RNA polymerase II transcript that represses the paternal expression of Ube3a. *Hum. Mol. Genet.*, **21**, 3001–3012.
36. Meng, L., Person, R.E., Huang, W., Zhu, P.J., Costa-Mattioli, M. and Beaudet, A.L. (2013) Truncation of Ube3a-ATS unsilences paternal Ube3a and ameliorates behavioral defects in the Angelman syndrome mouse model. *PLoS Genet.*, **9**, e1004039.
37. Jones, K.A., Han, J.E., DeBruyne, J.P. and Philpot, B.D. (2016) Persistent neuronal Ube3a expression in the suprachiasmatic nucleus of Angelman syndrome model mice. *Sci. Rep.*, **6**, 28238.
38. Aguilera, A. and Garcia-Muse, T. (2012) R loops: from transcription byproducts to threats to genome stability. *Mol. Cell*, **46**, 115–124.
39. Siepka, S.M., Yoo, S.H., Park, J., Song, W., Kumar, V., Hu, Y., Lee, C. and Takahashi, J.S. (2007) Circadian mutant overtime reveals F-box protein FBXL3 regulation of cryptochrome and period gene expression. *Cell*, **129**, 1011–1023.
40. Hutton, S.R. and Pevny, L.H. (2008) Isolation, culture, and differentiation of progenitor cells from the central nervous system. *Cold Spring Harb. Protoc.*, **3**, DOI: 10.1101/pdb.prot5077.
41. Katz, Y., Wang, E.T., Airoldi, E.M. and Burge, C.B. (2010) Analysis and design of RNA sequencing experiments for identifying isoform regulation. *Nat. Methods*, **7**, 1009–1015.
42. Katz, Y., Wang, E.T., Silterra, J., Schwartz, S., Wong, B., Thorvaldsdóttir, H., Robinson, J.T., Mesirov, J.P., Airoldi, E.M. and Burge, C.B. (2015) Quantitative visualization of alternative exon expression from RNA-seq data. *Bioinformatics*, **31**, 2400–2402.